

RECEIVED
AUG 04 1997
OSTI

ANL/PHY/CP-94/148
CONF-970622--

under Contract No. W-31-109-ENG-38 with the U.S. Department of Energy. The U.S. Government retains for itself, and others acting on its behalf, a paid-up, nonexclusive, irrevocable worldwide license in said article to reproduce, prepare derivative works, distribute copies to the public, and perform publicly and display publicly, by or on behalf of the Government.

1

Spin Distributions for $^{64}\text{Ni}+^{100}\text{Mo}$ with the Argonne/Notre Dame BGO-Array

D. Ackermann^{a,b}, B.B. Back^a, R.R. Betts^a, M. Carpenter^a, L. Corradi^b, S.M. Fischer^a, R. Ganz^a, S. Gil^c, G. Hackman^a, D.J. Hofman^a, R.V.F. Janssens^a, T.L. Khoo^a, G. Montagnoli^d, V. Nanal^a, F. Scarlassara^d, M. Schlapp^a, D. Seweryniak^a, A.M. Stefanini^b and A.H. Wuosmaa^a

^aArgonne National Laboratory, Argonne, Il, U.S.A

^bLaboratori Nazionali di Legnaro, Legnaro, Italy

^cDepartment of Physics, University Buenos Aires, Buenos Aires, Argentina

^dDepartment of Physics, University of Padova, Padova, Italy

The experimental representation of the fusion barrier distribution from the second derivative, $d^2(E\sigma_{\text{fus}})/dE^2$, was the basis for a series of precise measurements of the fusion excitation function. As an alternative approach, it has been proposed recently that the first derivative of the compound nucleus (CN) spin distribution is equivalent to $d^2(E\sigma_{\text{fus}})/dE^2$. Multiplicity distributions for the reactions $^{64}\text{Ni}+^{100}\text{Mo}$ and $^{32}\text{S}+^{110}\text{Pd}$ have been measured making use of the Argonne/Notre Dame-BGO-array and GASP, respectively. In particular, the influence of fission on the high spin tail of the spin distribution and the consequences for the experimental representation of the distribution of barriers is discussed for $^{64}\text{Ni}+^{100}\text{Mo}$.

1. Introduction

The investigation of subbarrier fusion has attracted renewed interest, following the partial success of the coupled channels approach in reproducing fusion cross sections. The experimental representation of the barrier distribution from the second derivative of the fusion cross section times energy, $d^2(E\sigma)/dE^2$ [1], has demonstrated the richness of information that may be obtained by precise measurements of the fusion excitation function. Excellent results have been obtained from investigations of the fusion of the spherical nucleus ^{16}O with the deformed ^{154}Sm target by Leigh et al. [2]. The measured barrier distribution was reproduced using deformation parameters β_2 and β_4 which are consistent with the values obtained from Coulomb excitation experiments.

Using the same approach, the influence of double phonon coupling on subbarrier fusion for $^{58}\text{Ni}+^{60}\text{Ni}$ has recently been shown [3] (fig. 1). The identification of these complex surface vibrations as the only relevant effects, and the negligible influence of other channels, in particular the 2n-transfer, have been substantiated by the comparison with the

DISTRIBUTION OF THIS DOCUMENT IS UNLIMITED

MASTER

DISCLAIMER

This report was prepared as an account of work sponsored by an agency of the United States Government. Neither the United States Government nor any agency thereof, nor any of their employees, makes any warranty, express or implied, or assumes any legal liability or responsibility for the accuracy, completeness, or usefulness of any information, apparatus, product, or process disclosed, or represents that its use would not infringe privately owned rights. Reference herein to any specific commercial product, process, or service by trade name, trademark, manufacturer, or otherwise does not necessarily constitute or imply its endorsement, recommendation, or favoring by the United States Government or any agency thereof. The views and opinions of authors expressed herein do not necessarily state or reflect those of the United States Government or any agency thereof.

DISCLAIMER

**Portions of this document may be illegible
in electronic image products. Images are
produced from the best available original
document.**

older $^{58}\text{Ni}+^{58}\text{Ni}$ data [4] which also show a characteristic double-peaked structure. This system has been investigated in order to look for the effects of transfer but instead, a signature of multiphonon coupling was found. Thus, the next logical step was to look for a clear case where effects other than surface vibrations can be excluded. ^{110}Pd is a vibrational nucleus with a well known two- and three-phonon structure. and we therefore decided to study the fusion of ^{110}Pd with $^{(32)}^{36}\text{S}$. The barrier distribution obtained from the measured fusion excitation function shows a characteristic structure which can be explained almost completely only by coupling up to the three-phonon states of ^{110}Pd [5]. This result shows, however, one of the limits of the technique of extracting the barrier distribution from differentiating twice the function $E \times \sigma_{\text{fus}}$. In the higher energy range, due to the large absolute cross sections and the flat slope, the experimental errors become large and the distribution is no longer well defined. This region, however, contains valid information for the understanding of the reaction process.

2. Spin Distribution as an Alternative

The second derivative of $E \times \sigma_{\text{fus}}$ can be viewed as a way to enhance in a limited energy-range around the Coulomb barrier features which might be hidden in the fusion excitation function. At very low energies, the logarithmic plot of the fusion excitation function magnifies effects that might be present better than the second derivative of $E \times \sigma_{\text{fus}}$ does. This is clearly shown e.g. by the comparison of the two systems $^{16,17}\text{O}+^{144}\text{Sm}$ measured by J. Leigh et al. [6]. Here, the difference between the two systems is more clearly visible in the logarithmic plot of the fusion excitation function than in the the second derivative. The high energy part of the fusion excitation function can be used as a good approximation for the average barrier by plotting the cross section values as a function of $1/E$ [7].

As an alternative approach it has been shown recently [8] that the first derivative of the compound nucleus (CN) spin distribution is equivalent to the barrier distribution obtained from the second derivative of $E \times \sigma_{\text{fus}}$. On the basis of the assumption

$$T_{\ell}(E, \ell) = T_0(E - E_{\text{rot}}(\ell)) \quad (1)$$

one can express the partial wave transmission probabilities [9] as

$$T_{\ell}(E, \ell) = \frac{1}{\pi R_b^2} \left(\frac{d(E\sigma_{\text{fus}})}{dE} \right). \quad (2)$$

The assumption (1) provides a transformation of the spin ℓ of the ℓ^{th} partial wave into an effective energy $E' = E - E_{\text{rot}}(\ell)$. With these ingredients one can derive the barrier distribution from a complete angular momentum distribution. In the first step one extracts the s -wave transmission function $T_0(E')$ transforming the spin values in effective energies E' and normalizing by the geometrical cross section for each partial wave ℓ :

$$T_{\ell}(E, \ell) = T_0(E' = E - E_{\text{rot}}(\ell), \ell = 0) = \frac{\sigma_{\ell}(E, \ell)}{(2\ell + 1)\pi\lambda^2}. \quad (3)$$

The derivative of this function gives according to eq. (2) the barrier distribution:

$$D(B) = \frac{1}{\pi R_b^2} \frac{d^2(E\sigma_{\text{fus}})}{dE^2} = \frac{dT_0(E')}{dE'}. \quad (4)$$

Thus, the partial wave distribution σ_ℓ at one energy E provides us with a transmission function and a barrier distribution spanning a range from E to $E - E_{\text{rot}}(\ell_{\text{max}})$. For instance, in the system $^{16}\text{O}+^{152}\text{Sm}$ at an energy above the barrier and a maximum angular momentum around $50\hbar$, one covers an energy range of 30-40 MeV which includes the entire barrier region. Wuosmaa et al. [10] measured for this system a set of spin distributions at various energies, in the range of the Coulomb barrier. The spin distribution measured at an energy above the Coulomb barrier and the barrier distribution extracted from those data using (3) and (4) are shown in fig. 2. One notes that the barrier distribution is consistent with what is expected for a deformed nucleus as e.g. in ref. [2].

To illustrate the complementarity of this technique, let's consider the very well studied fusion excitation function for $^{16}\text{O}+^{144}\text{Sm}$ measured by Leigh et al. [6]. A double peaked structure is seen in the second derivative of the measured fusion excitation function. The peaks are well defined and are located (6-7) MeV apart. However, at the second peak the errors become large because this structure is maximum at $E_{c.m.} \approx 66$ MeV, i.e. above the average barrier. In this region the slope of the fusion excitation function is nearly flat and obtaining meaningful information from the fusion cross section is difficult. This is precisely where a measurement of the spin distribution would help.

3. The Experiment

In a recent experiment γ -multiplicities have been measured for the systems $^{32}\text{S}+^{110}\text{Pd}$ and $^{16}\text{O}+^{152}\text{Sm}$ at the Ge-array GASP of the Laboratori Nazionali di Legnaro, Italy, in order to extract experimental barrier distributions from the derived spin distributions. The results should (1) prove the validity of the method and (2) complete the information of the coupling mechanism obtained from the previously measured fusion excitation function. The data are currently being analyzed. A second experiment on which we shall concentrate in this paper has been performed with a slightly different apparatus for the reaction $^{64}\text{Ni}+^{100}\text{Mo}$. Here, the Argonne/Notre Dame BGO-array at the Argonne National Laboratory ATLAS-facility has been used in conjunction with a combination of an electrostatic deflector and a Si-strip detector array.

The $^{64}\text{Ni}+^{100}\text{Mo}$ reaction has been subject of several previous experiments and the fusion cross sections around the barrier are known along with the average angular momenta [12,13]. The most recent investigation [12] claimed evidence for the importance of the one-plus-two phonon coupling, which should, on the other hand lead to a characteristic "experimental barrier distribution" similar to that obtained from experimental fusion excitation functions for $^{32}\text{S}+^{110}\text{Pd}$ and $^{58}\text{Ni}+^{60}\text{Ni}$.

The Argonne/Notre Dame BGO-array and GASP each have an efficiency of about 70%. The lower granularity of 50 detectors as compared with GASP's 80 BGO-crystals is still sufficient as the maximum multiplicities are around 25 (see fig. 3).

The main difference between the two setups is the way the evaporation-residue (ER) trigger was defined. Whereas in the GASP measurements characteristic γ -lines have been used for the ER-multiplicity coincidences, with the ANL/Notre Dame BGO-array the ER were detected directly in an array of four seven-strip Si-detectors with a total active area of (8×12) cm. The array was located at a distance of ≈ 1 m from the target behind the electrostatic deflector. The latter has the advantage of integrating over the whole ER-

distribution. Therefore, discontinuities due to the summing of different ER-channels in the spin distribution, as in principle possible in the GASP measurement, are avoided. On the other hand, some assumptions about the effects of particle evaporation must be made in the transformation from measured γ -ray multiplicity to spin (see discussion section 4).

4. Preliminary Results for $^{64}\text{Ni}+^{100}\text{Mo}$ and Interpretation

We measured γ -multiplicities for $^{64}\text{Ni}+^{100}\text{Mo}$ in coincidence with evaporation residues (ER) at three energies – $E_{\text{lab}} = 230$ MeV, 246 MeV and 260 MeV; i.e. at the barrier, at the point where fission becomes important and at an intermediate energy.

At all three energies we obtained ≈ 3700 counts for the total multiplicity spectrum. This rather low statistics was basically due to a background of scattered beam through the deflector which forced us to use a relatively low beam current. Nevertheless some conclusions can be drawn from the obtained multiplicity data which are shown in fig. 3a)-c). Preliminary spin distributions have been computed using a simple relation of the type

$$\ell = \Delta I_{\gamma ns}(M_{\gamma} - M_{\gamma s}) + \text{const}, \quad (5)$$

where M_{γ} denotes the measured γ -multiplicity, $\Delta I_{\gamma ns} = 2$ is the spin taken away by the yrast transitions and const contains the spin removed by statistical γ -rays ($M_{\gamma s}$), the particle evaporation and the ground state spin of the ER, using average values. This procedure is not correct for the lower spin region of the distribution, because the various evaporation channels are not equally distributed over the whole spin range. Therefore, the absolute spin-values should be taken with care. The shape of the higher end of the distribution, however, should not be affected. There we expect to observe the influence of the barrier distribution. For a large range of barriers a long tail should appear which at higher energies will be cut by fission. In fig. 4 a superposition of the spin distributions for the two highest energies is shown. One notes clearly a change in shape as illustrated by the cartoon in the same figure. The spin distribution taken at the lower energy has a relatively long tail of $> 22\hbar$, whereas the other one falls to zero over only $\approx 12\hbar$. The statistical errors, however, do not allow the extraction of the representation of barrier distributions with an accuracy sufficient to provide a detailed analysis of the coupling mechanism.

5. Conclusion and Outlook

In summary there are a few technical advantages in having a complete angular momentum distribution. Apart from fixing of the energy problem and covering a range of energies E' from $E_{\text{beam}} - E_{\text{rot}}(\ell_{\text{max}})$ to E_{beam} , measurements at different beam energies could be matched using the step-like transmission function (equation 3). (The position of the transition from 0 to 1 in $T_0(E')$ has to coincide in E' for the measurements at different energies.) In this way one could overcome also the limitation of having to measure at many fixed energy steps at intermediate energies.

Moreover, the measurement of a complete spin distribution is interesting in its own right. By providing information on the relative behavior of the single partial wave cross

sections, such a measurement contains more detailed information on the reaction mechanism around the Coulomb barrier than an integral fusion cross section measurement does.

In the present contribution, we have observed a long tail in the high spin region of the measured multiplicity (spin) distribution at energies at and slightly above the nominal Coulomb barrier. This suggests the presence of a rather broad distribution of barriers, as expected for a coupling scheme including several phonon states. At higher energies where fission sets in, this tail is truncated and no longer determined by the potential landscape of fusion, but rather by the energetic properties of the fission process. Better statistics are desirable in order to execute any detailed coupled channels analysis on the basis of the experimental representation of barriers. Much higher statistics have been accumulated for the reactions measured at GASP as can be seen for the 4n-channel of $^{32}\text{S}+^{110}\text{Pd}$ [14]. The much more complex data analysis is presently ongoing.

This work was carried out under the auspices of the U.S. Department of Energy under contract No. W-31-109-Eng-38.

REFERENCES

1. N. Rowley, G.R. Satchler and P.H. Stelson, *Phys. Lett.* **254B** (1991) p.21.
2. J.R. Leigh *et al.*, *Phys. Rev.* **C47** (1993) p.R437.
3. A.M. Stefanini *et al.*, *Phys. Rev. Lett.* **74** (1995) p.864.
4. M. Beckermann *et al.*, *Phys. Rev.* **C23** (1981) p.1581.
5. A.M. Stefanini *et al.*, *Phys. Rev.* **C52** (1995) p.R1727.
6. J.R. Leigh *et al.*, *Phys. Rev.* **C52** (1995) p.3151.
7. H.H. Gutbrod *et al.*, *Phys. Rev. Lett.* **30** (1973) p.398.
8. D. Ackermann, *Proc. "XXIX Zakopane School of Physics - Trends in Nuclear Physics", 5-14 September 1994, Zakopane, Poland, Acta Fisica Polonica* **B26** (1995) p.517.
9. C.C. Sahm *et al.*, *Nucl. Phys.* **A441** (1985) p.316.
10. A.H. Wuosmaa *et al.*, *Phys. Lett.* **B263** (1991) p.23.
11. D. Ackermann, Ph.D. thesis, TH Darmstadt, April 1995.
12. E. Rehm *et al.*, *Phys. Lett.* **B317** (1993) p.31.
13. M.L. Halbert *et al.*, *Phys. Rev.* **C40** (1989) p.2558.
14. D. Ackermann *et al.*, *Proc. "FUSION97, International Workshop on Heavy-Ion Collisions at Near-Barrier Energies", 17-21 March 1997, South Durras, Australia, to be published in Jour. of Phys G.*

Figurecaptions

- Fig.1 The experimental barrier distribution for $^{58}\text{Ni}+^{60}\text{Ni}$ compared with coupled channel calculations in the one-, two-, three- and four-phonon-channel spaces generated by considering up to mutual double excitation. (From ref. [3])
- Fig.2 Experimental angular momentum distribution for $^{16}\text{O}+^{152}\text{Sm}$ at a beam energy of $E_{\text{lab}} = 80$ MeV [10] (left panel) and barrier distribution (right panel) extracted from it. (From ref. [11])
- Fig.3 γ -multiplicity (a-c) and spin distributions (d-f) for the reaction $^{64}\text{Ni}+^{100}\text{Mo}$ at three energies (see text)
- Fig.4 Comparison of the spin distributions at the two higher energies (fig.3 e and f)

fig. 4

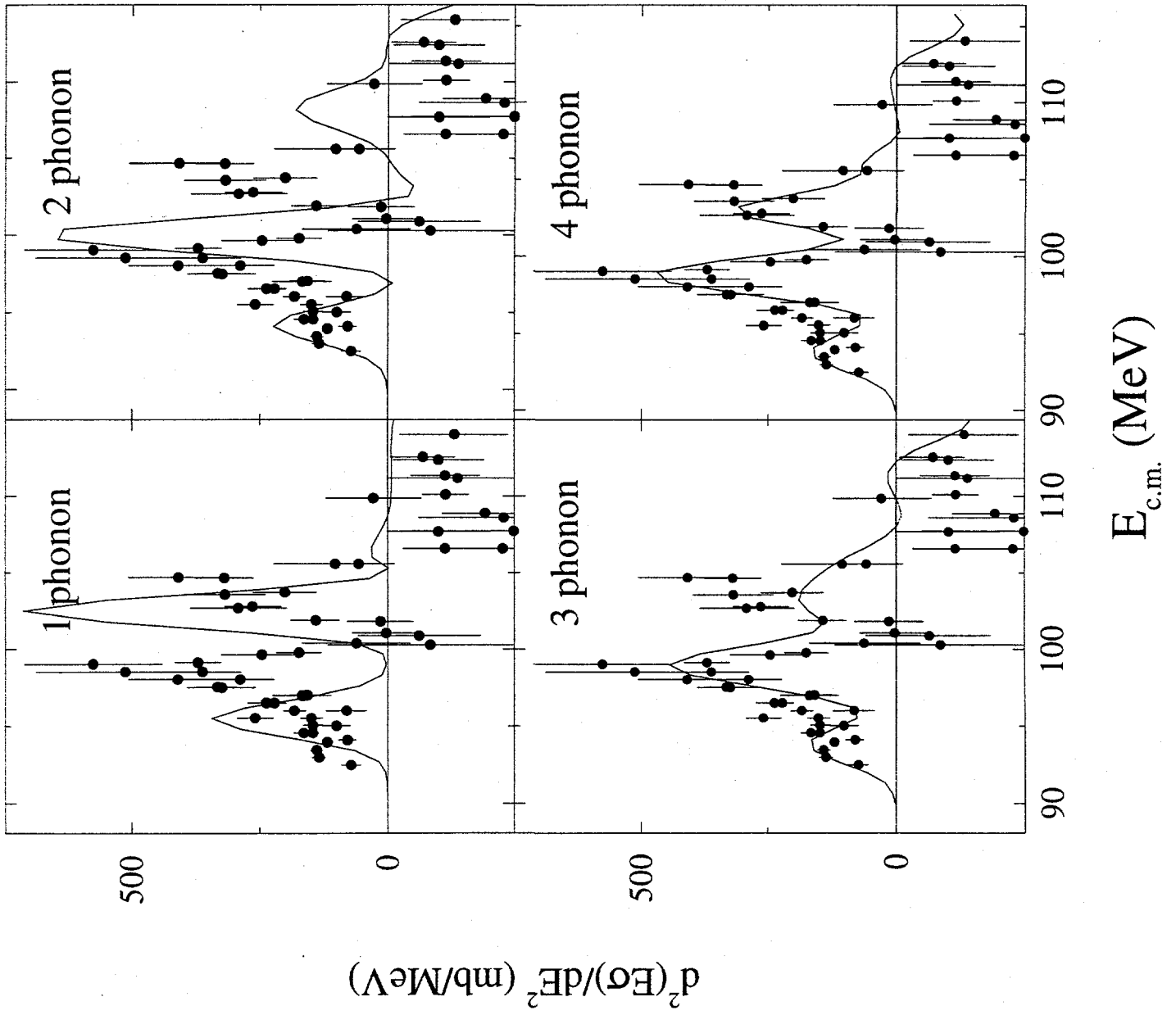


Fig 2

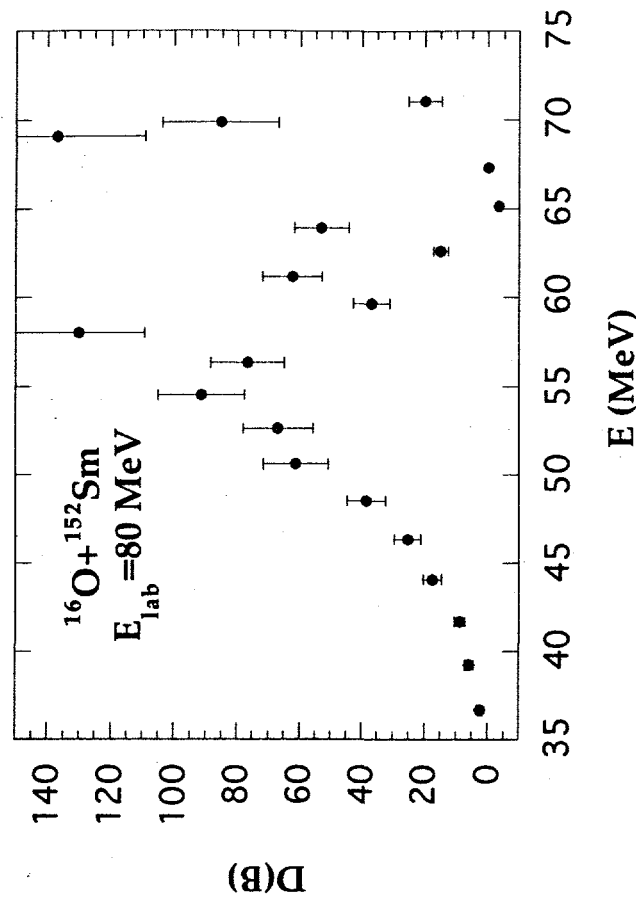
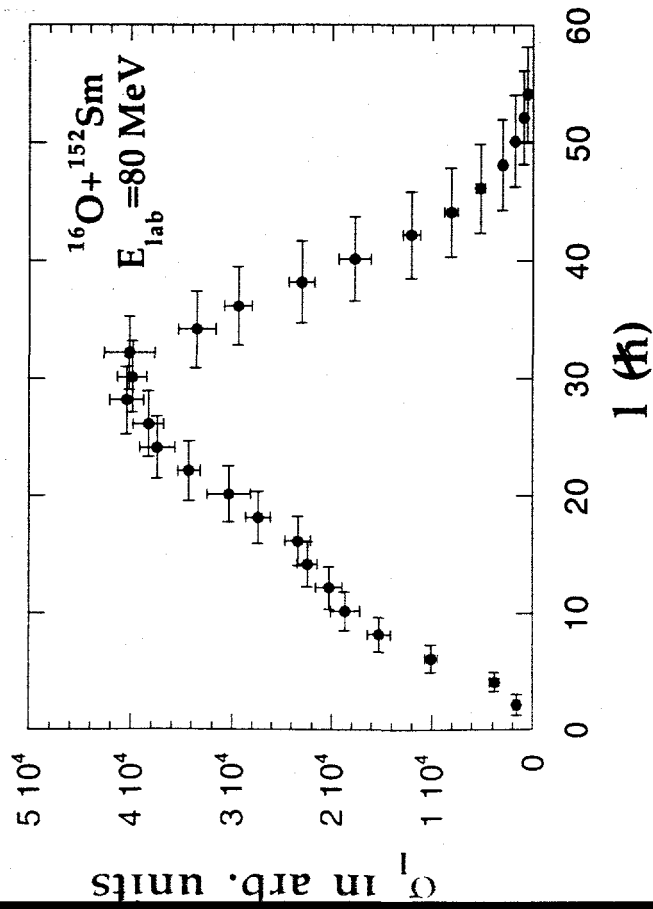


fig 3

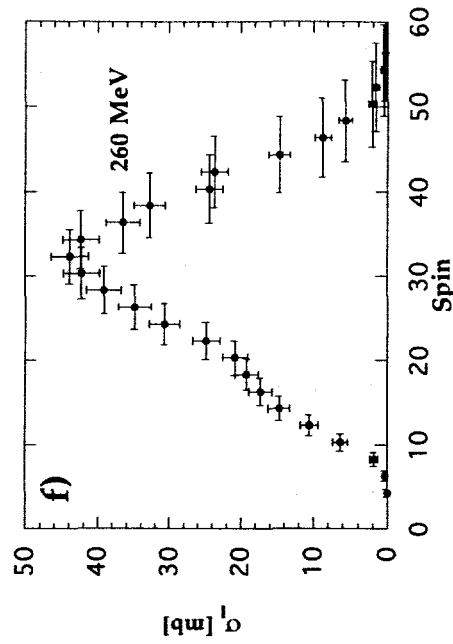
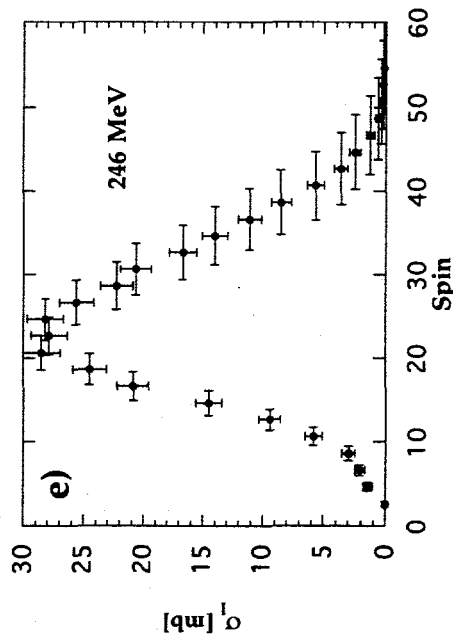
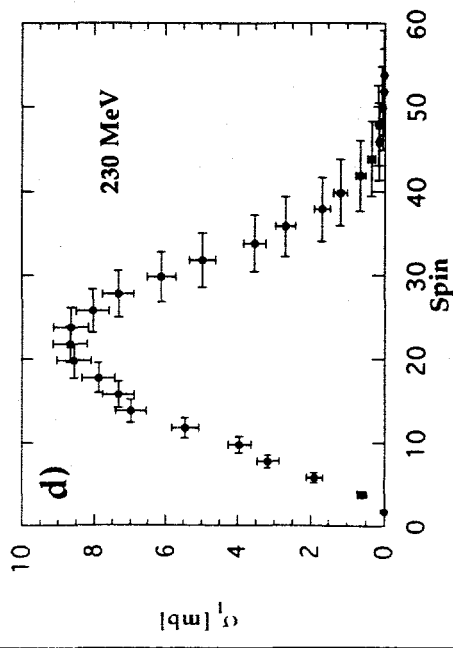
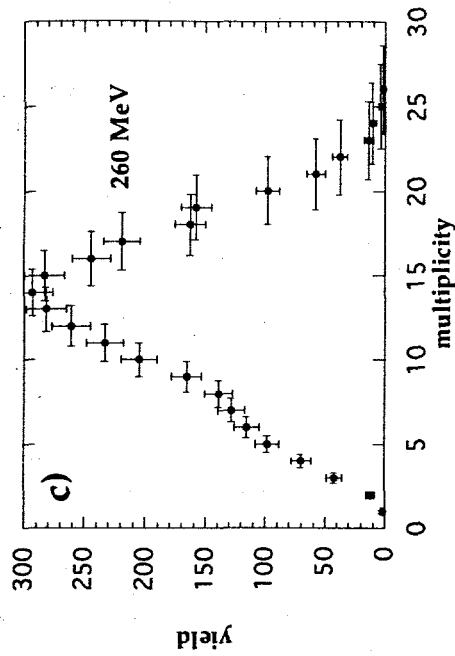
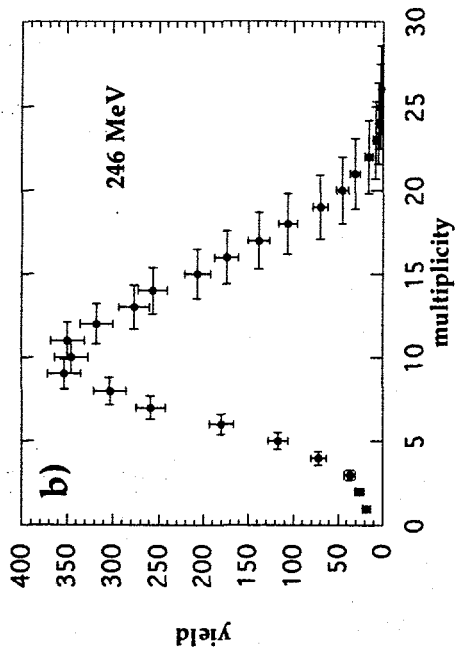
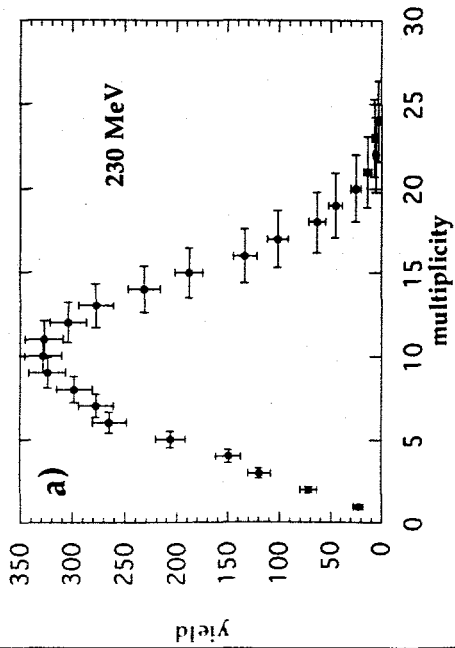


fig 4 left

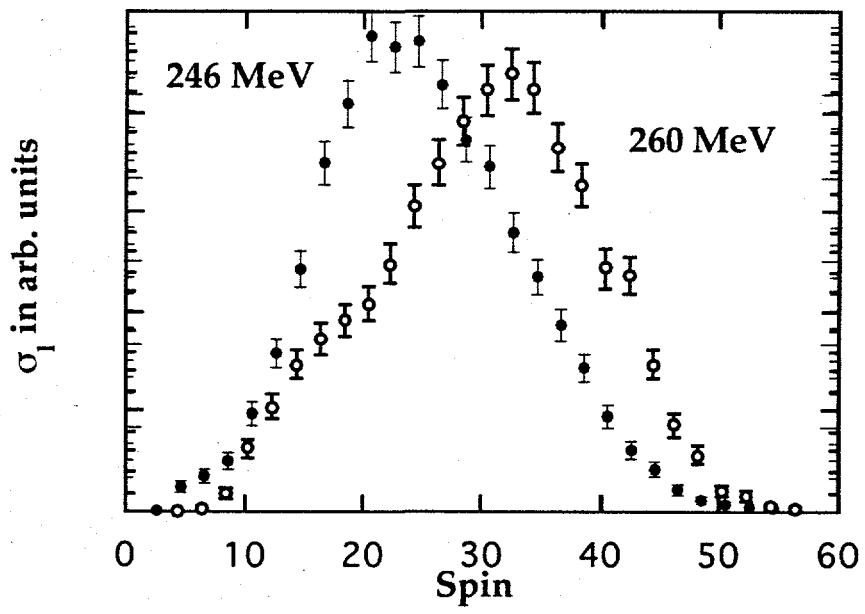


Fig 4 right

